

A mathematical and numerical framework for near-field optics*

Habib Ammari[†] Doo Sung Choi[‡] Sanghyeon Yu[†]

Abstract

This paper is concerned with the inverse problem of reconstructing small and local perturbations of a planar surface using the field interaction between a known plasmonic particle and the planar surface. The aim is to perform a super-resolved reconstruction of these perturbations from shifts in the plasmonic frequencies of the particle-surface system. In order to analyze the interaction between the plasmonic particle and the planar surface, a well chosen conformal mapping, which transforms the particle-surface system into a coated structure, is used. Then the even Fourier coefficients of the transformed domain are related to the shifts in the plasmonic resonances of the particle-surface system. A direct reconstruction of the perturbations of the planar surface is proposed. Its viability and limitations are documented by numerical examples.

Mathematics Subject Classification (MSC2000): 35R30, 35C20.

Key words. Near-field optics, plasmonic sensing, super-resolution, Möbius transformation, generalized polarization tensors, plasmonic resonances.

1 Introduction

In conventional optical imaging and spectroscopy, a sample is typically illuminated by a light source and the scattered light is recorded by a detector. The formed images are diffraction-limited. The diffraction limit essentially means that visible light cannot image nanomaterials.

In near-field optics, by placing a probe to exploit the unique properties of metal nanostructures at optical frequencies to localize incident illumination and enhance the light-matter interaction on the sample, one breaks the resolution limit [17, 18, 19, 20, 21, 22, 30, 31]. Typically, the probe is a resonant plasmonic nanoparticle. At resonant frequencies, a light wave incident on the plasmonic probe gives rise to a greatly amplified electric field just outside the probe, which then affects the nearby sample [30, 31]. When the plasmonic

*The work of D. S. Choi is supported by the Korean Ministry of Science, ICT and Future Planning through NRF grant No. 2016R1A2B4014530.

[†]Department of Mathematics, ETH Zürich, Rämistrasse 101, CH-8092 Zürich, Switzerland (habib.ammari@math.ethz.ch, sanghyeon.yu@sam.math.ethz.ch).

[‡]Department of Mathematical Sciences, Korea Advanced Institute of Science and Technology, Daejeon 34141, South Korea (7john@kaist.ac.kr).

probe scans the sample surface one can form an image with a resolution much smaller than the diffraction limit by measuring the shifts of the plasmonic resonance induced by local defects for different particle's positions. The physical mechanism is based on the excitation of plasmonic modes at the same particular frequencies as the nanoprobe and their coupling with the evanescent light. The plasmonic particle interacts with the surface and propagates its near field information into the far-field [12, 13, 14, 30, 31] through the introduced shifts in its plasmonic resonances.

The plasmon resonant frequency is one of the most important characteristics of a plasmonic particle. It depends not only on the electromagnetic properties of the particle and its size and shape [8, 9, 27, 32], but also on the electromagnetic properties of the environment [8, 27, 29]. It is the last property which enables sensing applications of plasmonic particles [29].

In this paper, we first provide a mathematical and computational framework to elucidate physical mechanisms for going beyond the diffraction limit in near-field optics based on the excitation of surface plasmons. We mathematically and numerically analyze the intriguing behavior of light under the influence of plasmonics which allows nano-sensing of samples by using a localized surface plasmonic mode at the nanoprobe. We consider a plasmonic nanoparticle placed near a locally perturbed planar surface. We propose a mathematical and numerical framework to quantitatively image the sample from shifts in the plasmonic resonances due to the coupling between the nanoparticle and the perturbed planar surface. The key idea is to use a well-chosen conformal mapping and to express the far-field and the shifts in the plasmonic resonances in terms of the Fourier coefficients of the transformed domain. We compare the reconstructed images to those obtained from the contracted generalized polarization tensors of the transformed domain, which are the gold standard in wave imaging of small particles [2, 6, 7, 10].

It is worth emphasizing that the physical system in which our method is realized is a plasmonic nanoparticle in the vicinity of a planar surface. The physical systems for imaging sub-wavelength surface defects described in [21, 22] can be mapped onto such a configuration. Moreover, in near-field optics, besides the method based on excitation of surface plasmon described in this paper, there have been a variety of attempts to attain super-resolution imaging. These include resonant energy transfer between fluorescence molecules and metallic or dielectric particles and interfaces and the generation or conversion of an evanescent wave at a grating with a period finer than the operating wavelength. We refer the interested reader to, for instance, [25] for an overview of these super-resolution methods in optics.

Our results in this work extend those in [10, 11], where a two particle system is considered. In [10, 11], the system is composed of a known plasmonic particle and a small object. By varying the relative position of the particles, it is shown that fine details of the shape of the small object can be reconstructed from the induced shifts of the plasmonic resonant frequencies of the plasmonic particle.

The paper is organized as follows. In Section 2, we provide basic results on layer potentials and then explain the concepts of plasmonic resonances and contracted generalized polarization tensors. In Section 3, we consider the forward scattering problem of the incident field interaction with a system composed of a plasmonic particle and a perturbed planar surface. We apply a Möbius transformation in order to transform the plasmonic particle and the half-plane into concentric disks. Then we derive the asymptotic expan-

sions of the scattered field and the plasmonic resonances of the particle-surface system. In Section 4, we consider the inverse problem of reconstructing the perturbations of the planar surface. This is done by relating the shifts in the resonances of the particle-planar surface system to the Fourier coefficients of the transformed domain. In Section 5, we provide numerical examples to justify our theoretical results and to illustrate the performances of the proposed Fourier-based reconstruction scheme. In particular, we compare the reconstructed images to those obtained from the contracted generalized polarization tensors of the transformed domain.

2 Preliminary results

2.1 Layer potentials

We recall some basic results from layer potential theory that are needed for subsequent analysis. We refer to [4] for more details. We denote by $\Gamma(\mathbf{x}, \mathbf{y})$ the fundamental solution of the Laplacian in \mathbb{R}^2 , i.e.,

$$\Gamma(\mathbf{x}, \mathbf{y}) = \frac{1}{2\pi} \ln |\mathbf{x} - \mathbf{y}|.$$

Let D be a bounded domain in \mathbb{R}^2 with $\mathcal{C}^{1,\eta}$ boundary for some $\eta > 0$, and let $\nu(\mathbf{x})$ be the outward normal for $\mathbf{x} \in \partial D$.

The single-layer potential \mathcal{S}_D associated with D is defined by

$$\mathcal{S}_D[\varphi](\mathbf{x}) = \int_{\partial D} \Gamma(\mathbf{x}, \mathbf{y}) \varphi(\mathbf{y}) d\sigma(\mathbf{y}), \quad \mathbf{x} \in \mathbb{R}^2,$$

and the Neumann-Poincaré (NP) operator \mathcal{K}_D^* by

$$\mathcal{K}_D^*[\varphi](\mathbf{x}) = \int_{\partial D} \frac{\partial \Gamma}{\partial \nu(\mathbf{x})}(\mathbf{x}, \mathbf{y}) \varphi(\mathbf{y}) d\sigma(\mathbf{y}), \quad \mathbf{x} \in \partial D.$$

The following jump relations hold:

$$\mathcal{S}_D[\varphi]|_+ = \mathcal{S}_D[\varphi]|_-, \tag{2.1}$$

$$\frac{\partial \mathcal{S}_D[\varphi]}{\partial \nu} \Big|_{\pm} = (\pm \frac{1}{2} I + \mathcal{K}_D^*)[\varphi]. \tag{2.2}$$

Here, the subscripts $+$ and $-$ indicate the limits from outside and inside D , respectively.

Let $H^{1/2}(\partial D)$ be the usual Sobolev space and let $H^{-1/2}(\partial D)$ be its dual space with respect to the duality pairing $(\cdot, \cdot)_{-\frac{1}{2}, \frac{1}{2}}$. We denote by $H_0^{-1/2}(\partial D)$ the collection of all $\varphi \in H^{-1/2}(\partial D)$ such that $(\varphi, 1)_{-\frac{1}{2}, \frac{1}{2}} = 0$.

The NP operator is bounded from $H^{-1/2}(\partial D)$ into $H^{-1/2}(\partial D)$. Moreover, the operator $\lambda I - \mathcal{K}_D^* : L^2(\partial D) \rightarrow L^2(\partial D)$ is invertible for any $|\lambda| > 1/2$ [4, 26]. Although the NP operator is not self-adjoint on $L^2(\partial D)$, it can be symmetrized on $H_0^{-1/2}(\partial D)$ with a proper inner product [15, 8]. In fact, let $\mathcal{H}^*(\partial D)$ be the space $H_0^{-1/2}(\partial D)$ equipped with the inner product $(\cdot, \cdot)_{\mathcal{H}^*(\partial D)}$ defined by

$$(\varphi, \psi)_{\mathcal{H}^*(\partial D)} = -(\varphi, \mathcal{S}_D[\psi])_{-\frac{1}{2}, \frac{1}{2}}, \tag{2.3}$$

for $\varphi, \psi \in H^{-1/2}(\partial D)$. Then using the Plemelj's symmetrization principle,

$$\mathcal{S}_D \mathcal{K}_D^* = \mathcal{K}_D \mathcal{S}_D,$$

it can be shown that the NP operator \mathcal{K}_D^* is self-adjoint in \mathcal{H}^* with the inner product $(\cdot, \cdot)_{\mathcal{H}^*(\partial D)}$ [15, 28]. Since \mathcal{K}_D^* is also compact, it admits the following spectral decomposition in \mathcal{H}^* ,

$$\mathcal{K}_D^* = \sum_{j=1}^{\infty} \lambda_j (\cdot, \varphi_j)_{\mathcal{H}^*} \varphi_j, \quad (2.4)$$

where λ_j are the eigenvalues of \mathcal{K}_D^* and φ_j are their associated eigenfunctions. Note that $|\lambda_j| < 1/2$ for all $j \geq 1$.

2.2 Plasmonic resonances of metallic particles

In this subsection, we are interested in the frequency regime where plasmonic resonances occur in free space. In such a regime, the wavelength of the incident field is much greater than the size of the plasmonic particle. To simplify the analysis and better illustrate the main idea, we use the quasi-static approximation (by assuming the incident wavelength to be infinite) to model the interaction. More precisely, let Ω represent a plasmonic particle with permittivity ε_c embedded in the homogeneous space \mathbb{R}^2 with permittivity ε_0 . We consider the following transmission problem with given incident field u^i which is harmonic in \mathbb{R}^2 :

$$\begin{cases} \nabla \cdot (\varepsilon \nabla u) = 0 & \text{in } \mathbb{R}^2, \\ (u - u^i)(\mathbf{x}) = O(|\mathbf{x}|^{-1}) & \text{as } |\mathbf{x}| \rightarrow \infty, \end{cases} \quad (2.5)$$

where $\varepsilon = \varepsilon_c \chi(\Omega) + \varepsilon_0 \chi(\mathbb{R}^2 \setminus \overline{\Omega})$, and $\chi(\Omega)$ and $\chi(\mathbb{R}^2 \setminus \overline{\Omega})$ are the characteristic functions of Ω and $\mathbb{R}^2 \setminus \overline{\Omega}$, respectively. The problem (2.5) describes the response of the plasmonic particle Ω to the illumination u^i in the quasi-static limit.

The total field u outside of Ω can be represented by (see [15])

$$u = u^i + \mathcal{S}_\Omega[\varphi], \quad (2.6)$$

where the density φ satisfies the boundary integral equation

$$(\lambda I - \mathcal{K}_\Omega^*)[\varphi] = \frac{\partial u^i}{\partial \nu} \Big|_{\partial \Omega}. \quad (2.7)$$

Here, the permittivity contrast λ is given by

$$\lambda = \frac{\varepsilon_c + \varepsilon_0}{2(\varepsilon_c - \varepsilon_0)}. \quad (2.8)$$

Contrary to ordinary dielectric particles, the permittivity ε_c of the plasmonic particle has negative real parts. In fact, ε_c depends on the operating frequency ω and can be modeled by the following Drude's model

$$\varepsilon_c = \varepsilon_c(\omega) = \varepsilon_0 \left(1 - \frac{\omega_p^2}{\omega(\omega + i\gamma)} \right), \quad (2.9)$$

where $\omega_p > 0$ is called the plasma frequency and $\gamma > 0$ is the damping parameter. Since the parameter γ is typically very small, $\varepsilon_c(\omega)$ has a small imaginary part.

Now we discuss the plasmonic resonances. By applying the spectral decomposition (2.4) of \mathcal{K}_Ω^* to the integral equation (2.7), we obtain

$$u = u^i + \sum_{j=1}^{\infty} \frac{(\frac{\partial u^i}{\partial \nu}, \varphi_j)_{\mathcal{H}^*(\partial\Omega)}}{\lambda - \lambda_j} \mathcal{S}_\Omega[\varphi_j].$$

Recall that λ_j are eigenvalues \mathcal{K}_Ω^* and they satisfy the condition that $|\lambda_j| < 1/2$. For $\omega < \omega_p$, $\Re[\varepsilon_c(\omega)]$ can take negative values. Then it holds that $|\Re[\lambda(\omega)]| < 1/2$. If there exists a frequency, say ω_j , such that $\lambda(\omega_j)$ is close to an eigenvalue λ_j of the NP operator and their difference is locally minimized. Provided that $(\frac{\partial u^i}{\partial \nu}, \varphi_j)_{\mathcal{H}^*(\partial\Omega)} \neq 0$, the eigenmode φ_j in (2.2) will be fully excited and it dominates over other modes. As a result, the scattered field $u - u^i$ will show a pronounced peak at the frequency ω_j . This phenomenon is called the plasmonic resonance and ω_j is called the plasmonic resonant frequency. We refer the reader to [15, 16, 8] for the details.

We also mention that, for a precise reconstruction, the plasmonic particles with low-loss. In other words, the damping parameter should be small. It is known that silver and gold have relatively low loss. If loss is high, then the location of resonant peaks can be quite different from the one corresponding to the eigenvalue λ_j .

2.3 Contracted generalized polarization tensors

In this subsection, we explain the concept of the generalized polarization tensors (GPTs) associated with a smooth bounded domain D having a permittivity ϵ_D . Let u be the solution of (2.5) and let λ_D be defined by (2.8) with ε_c replaced by ε_D . The scattered field $u - u^i$ has the following far-field behavior [4, p. 77]

$$(u - u^i)(\mathbf{x}) = \sum_{|\alpha|, |\beta| \leq 1} \frac{(-1)^{|\beta|}}{\alpha! \beta!} \partial^\alpha u^i(0) M_{\alpha\beta}(\lambda_D, D) \partial^\beta \Gamma(\mathbf{x}), \quad |\mathbf{x}| \rightarrow +\infty,$$

where $M_{\alpha\beta}(\lambda_D, D)$ is given by

$$M_{\alpha\beta}(\lambda_D, D) := \int_{\partial D} y^\beta (\lambda_D I - \mathcal{K}_D^*)^{-1} \left[\frac{\partial \mathbf{x}^\alpha}{\partial \nu} \right](\mathbf{y}) d\sigma(\mathbf{y}), \quad \alpha, \beta \in \mathbb{N}^2.$$

Here, the coefficient $M_{\alpha\beta}(\lambda_D, D)$ is called the *generalized polarization tensor* [4].

For $m \in \mathbb{N}$, let $P_m(\mathbf{x})$ be the complex-valued polynomial

$$P_m(\mathbf{x}) = r^m \cos m\theta + ir^m \sin m\theta, \quad (2.10)$$

with $\mathbf{x} = re^{i\theta}$ in the polar coordinates. For n and m in \mathbb{N} , we define the *contracted generalized polarization tensors* (CGPTs) to be the following linear combinations of generalized

polarization tensors using the homogeneous harmonic polynomials introduced in (2.10):

$$\begin{aligned}
M_{mn}^{cc}(\lambda_D, D) &= \int_{\partial D} \Re[P_n](\lambda_D I - \mathcal{K}_D^*)^{-1} \left[\frac{\partial \Re[P_m]}{\partial \nu} \right] d\sigma, \\
M_{mn}^{cs}(\lambda_D, D) &= \int_{\partial D} \Im[P_n](\lambda_D I - \mathcal{K}_D^*)^{-1} \left[\frac{\partial \Re[P_m]}{\partial \nu} \right] d\sigma, \\
M_{mn}^{sc}(\lambda_D, D) &= \int_{\partial D} \Re[P_n](\lambda_D I - \mathcal{K}_D^*)^{-1} \left[\frac{\partial \Im[P_m]}{\partial \nu} \right] d\sigma, \\
M_{mn}^{ss}(\lambda_D, D) &= \int_{\partial D} \Im[P_n](\lambda_D I - \mathcal{K}_D^*)^{-1} \left[\frac{\partial \Im[P_m]}{\partial \nu} \right] d\sigma.
\end{aligned} \tag{2.11}$$

We remark that the CGPTs defined above encode useful information about the shape of the particle D and can be used for its reconstruction. See [3, 4, 5, 7] for more details.

It is sometimes more convenient to use the complex version of the contracted GPTs defined by

$$\mathbb{N}_{nm}^{(1)} := M_{nm}^{cc} - M_{nm}^{ss} + i(M_{nm}^{cs} + M_{nm}^{sc}), \tag{2.12}$$

$$\mathbb{N}_{nm}^{(2)} := M_{nm}^{cc} + M_{nm}^{ss} - i(M_{nm}^{cs} - M_{nm}^{sc}), \tag{2.13}$$

for $n, m \neq 0$. Here, M_{nm}^{cc} , M_{nm}^{ss} , M_{nm}^{cs} , and M_{nm}^{sc} are defined by (2.11).

2.4 Shape derivatives of CGPTs

Let D_δ be a small perturbation of the domain D defined as follows: there is $h \in \mathcal{C}(\partial D)$ such that ∂D_δ is given by

$$\partial D_\delta = \{\mathbf{x} + \delta h(\mathbf{x})\nu(\mathbf{x}) : \mathbf{x} \in \partial D\}. \tag{2.14}$$

Then we have the following formula for the shape perturbation of the complex GPTs [2, 3]:

$$\begin{aligned}
&\mathbb{N}_{nm}^{(2)}(\lambda_D, D_\delta) - \mathbb{N}_{nm}^{(2)}(\lambda_D, D) \\
&= \delta \left(\frac{\varepsilon_D}{\varepsilon_0} - 1 \right) \int_{\partial D_0} h(\mathbf{x}) \left[\frac{\partial u_n}{\partial \nu} \Big|_- \frac{\partial v_{-m}}{\partial \nu} \Big|_- + \frac{\varepsilon_0}{\varepsilon_D} \frac{\partial u_n}{\partial T} \Big|_- \frac{\partial v_{-m}}{\partial T} \Big|_- \right] (\mathbf{x}) d\sigma(\mathbf{x}) + O(\delta^2),
\end{aligned}$$

where u_n and v_m are respectively the solutions to the following transmission problems:

$$\begin{cases} \Delta u = 0 & \text{in } \mathbb{R}^2 \setminus \partial D, \\ u|_+ = u|_- & \text{on } \partial D, \\ \varepsilon_0 \frac{\partial u}{\partial \nu} \Big|_+ = \varepsilon_D \frac{\partial u}{\partial \nu} \Big|_- & \text{on } \partial D, \\ (u - H)(\mathbf{x}) = O(|\mathbf{x}|^{-1}) & \text{as } |\mathbf{x}| \rightarrow \infty, \end{cases} \tag{2.15}$$

and

$$\begin{cases} \Delta v = 0 & \text{in } \mathbb{R}^2 \setminus \partial D, \\ \varepsilon_D v|_+ = \varepsilon_0 v|_- & \text{on } \partial D, \\ \frac{\partial v}{\partial \nu} \Big|_- = \frac{\partial v}{\partial \nu} \Big|_+ & \text{on } \partial D, \\ (v - F)(\mathbf{x}) = O(|\mathbf{x}|^{-1}) & \text{as } |\mathbf{x}| \rightarrow \infty, \end{cases} \tag{2.16}$$

with $H(\mathbf{x}) = r^{|n|} e^{in\theta}$ and $F(\mathbf{x}) = r^{|m|} e^{im\theta}$.

When D is the unit disk, the shape derivative can be computed explicitly. One can easily see that the solutions u_n and v_m of (2.15) and (2.16) are given by

$$u_n(\mathbf{x}) = \begin{cases} \frac{2\varepsilon_0}{\varepsilon_0 + \varepsilon_D} r^{|n|} e^{in\theta} & \text{if } |\mathbf{x}| = r < 1, \\ \left(r^{|n|} + \frac{\varepsilon_0 - \varepsilon_D}{\varepsilon_0 + \varepsilon_D} r^{-|n|} \right) e^{in\theta} & \text{if } |\mathbf{x}| = r > 1, \end{cases} \quad (2.17)$$

and

$$v_m(\mathbf{x}) = \begin{cases} \frac{2\varepsilon_D}{\varepsilon_0 + \varepsilon_D} r^{|m|} e^{im\theta} & \text{if } |\mathbf{x}| = r < 1, \\ \left(r^{|m|} + \frac{\varepsilon_0 - \varepsilon_D}{\varepsilon_0 + \varepsilon_D} r^{-|m|} \right) e^{im\theta} & \text{if } |\mathbf{x}| = r > 1. \end{cases} \quad (2.18)$$

Then, in view of (2.4), we obtain the following result.

Lemma 2.1. *For $n, m \neq 0$,*

$$\mathbb{N}_{nm}^{(2)}(\lambda_D, D_\delta) - \mathbb{N}_{nm}^{(2)}(\lambda_D, D) = \delta \frac{2\pi(\varepsilon_D |nm| + \varepsilon_0 nm)}{(\varepsilon_D - \varepsilon_0) \lambda_{-+}^2} \hat{h}(-n + m) + O(\delta^2), \quad (2.19)$$

where λ_D is given as $\lambda_D = (\varepsilon_D + \varepsilon_0)/(2(\varepsilon_D - \varepsilon_0))$ and $\hat{h}(k)$ is the Fourier coefficient of $h(\theta) := h(\cos \theta, \sin \theta)$ defined by

$$\hat{h}(k) = \frac{1}{2\pi} \int_0^{2\pi} h(\theta) e^{-ik\theta} d\theta.$$

For later use, we note that

$$\hat{h}(-k) = \overline{\hat{h}(k)} \quad (2.20)$$

for all $k \in \mathbb{N}$, which follows from the fact that h is a real-valued function.

3 The forward problem

In this section, we consider a plasmonic nanoparticle placed close to a locally perturbed planar surface. We let \mathbb{H}_0 to be the (unperturbed) lower half-plane

$$\mathbb{H}_0 = \{\mathbf{x} \in \mathbb{R}^2 : \mathbf{x} = (x_1, x_2), \quad x_2 < 0\}$$

with $\partial\mathbb{H}_0 = \{\mathbf{x} \in \mathbb{R}^2 : \mathbf{x} = (x_1, 0)\}$ being its boundary.

We define \mathbb{H}_δ to be a δ -perturbation of \mathbb{H}_0 , *i.e.*, we let $h_0 \in \mathcal{C}(\partial\mathbb{H}_0)$ and $\partial\mathbb{H}_\delta$ be given by

$$\partial\mathbb{H}_\delta = \{\mathbf{x} + \delta h_0(\mathbf{x}) \nu(\mathbf{x}) : \mathbf{x} \in \partial\mathbb{H}_0\},$$

where

$$\text{supp}(h_0) \subset [-R, R] \quad \text{for some } R > 0. \quad (3.1)$$

We assume that δ is a small positive parameter and R is of order one.

We also define a plasmonic particle Ω :

$$\Omega = \{\mathbf{x} \in \mathbb{R}^2 : |\mathbf{x} - (0, d)| < r_\Omega\},$$

where r_Ω is the radius of the plasmonic particle and d is the distance between the center of Ω and \mathbb{H}_0 . Assume that they are of order one, *i.e.*, $r_\Omega, d = O(1)$.

3.1 Transmission problem in the perturbed half-space

We consider the following transmission problem:

$$\begin{cases} \nabla \cdot (\varepsilon \nabla u) = 0 & \text{in } \mathbb{R}^2 \setminus (\partial \mathbb{H}_\delta \cup \partial \Omega), \\ u|_+ = u|_- & \text{on } \partial \mathbb{H}_\delta \cup \partial \Omega, \\ \varepsilon_+ \frac{\partial u}{\partial \nu} \Big|_+ = \varepsilon_- \frac{\partial u}{\partial \nu} \Big|_- & \text{on } \partial \mathbb{H}_\delta, \\ \varepsilon_+ \frac{\partial u}{\partial \nu} \Big|_+ = \varepsilon_c \frac{\partial u}{\partial \nu} \Big|_- & \text{on } \partial \Omega, \\ (u - u^i)(\mathbf{x}) = O(|\mathbf{x}|^{-1}) & \text{as } |\mathbf{x}| \rightarrow \infty, \end{cases} \quad (3.2)$$

where $\varepsilon = \varepsilon_- \chi(\mathbb{H}_\delta) + \varepsilon_+ \chi(\mathbb{R}^2 \setminus (\mathbb{H}_\delta \cup \Omega)) + \varepsilon_c \chi(\Omega)$ with $\varepsilon_-, \varepsilon_+ > 0$. Here, $u^i = -\mathbf{a} \cdot \mathbf{x}$ represents the potential of a uniform incident field in the direction $\mathbf{a} \in \mathbb{R}^2$.

To capture the interaction between the half-space and the plasmonic particle, we use a conformal mapping technique. Define the conformal transformation Φ , for $(x_1, x_2) \in \mathbb{R}^2$, by

$$\Phi(z) = \frac{z + i\sqrt{d^2 - r_\Omega^2}}{z - i\sqrt{d^2 - r_\Omega^2}}, \quad z = x_1 + ix_2.$$

Then \mathbb{H}_δ and $\mathbb{R}^2 \setminus \overline{\Omega}$ are transformed into the domains

$$D_{1,\delta} := \Phi(\mathbb{H}_\delta) \text{ and } D_2 := \Phi(\mathbb{R}^2 \setminus \overline{\Omega}) = \{|\zeta| < e^s\},$$

where the parameter $s > 0$ is given by

$$\sinh s = (\sqrt{(d/r_\Omega)^2 - 1}).$$

Note that the domain $D_{1,\delta}$ becomes the unit disk when $\delta = 0$, *i.e.*,

$$D_{1,0} = \Phi(\mathbb{H}_0) = \{|\zeta| < 1\}.$$

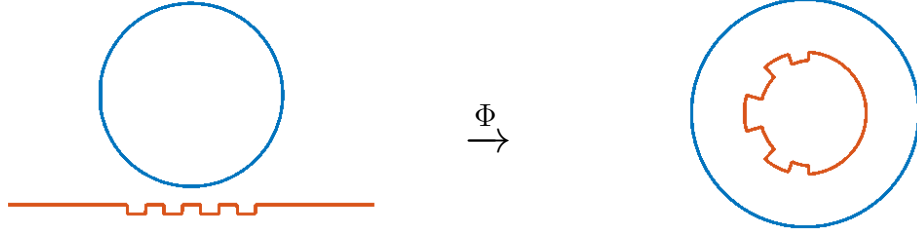
Since $D_{1,\delta}$ is a δ -perturbation of $D_{1,0}$, there is $h \in \mathcal{C}(\partial D_{1,0})$ such that $\partial D_{1,\delta}$ is given by

$$\partial D_{1,\delta} = \{\mathbf{x} + \delta h(\mathbf{x})\nu(\mathbf{x}) : \mathbf{x} \in \partial D_{1,0}\} = \{e^{i\theta} + \delta h(\theta)e^{i\theta} : \theta \in [0, 2\pi)\}. \quad (3.3)$$

Figure 3.1 describes the transforming system of the whole domain.

For convenience, we denote $D_{1,\delta}$ by D_1 . Since the mapping Φ is conformal, it can be shown that the transformed potential $\tilde{u}(\zeta) := u(\Phi^{-1}(\zeta))$ satisfies the following transmission problem:

$$\begin{cases} \nabla \cdot (\varepsilon \nabla \tilde{u}) = 0 & \text{in } \mathbb{R}^2 \setminus (\partial D_1 \cup \partial D_2), \\ \tilde{u}|_+ = \tilde{u}|_- & \text{on } \partial D_1 \cup \partial D_2, \\ \varepsilon_+ \frac{\partial \tilde{u}}{\partial \nu_1} \Big|_+ = \varepsilon_- \frac{\partial \tilde{u}}{\partial \nu_1} \Big|_- & \text{on } \partial D_1, \\ \varepsilon_c \frac{\partial \tilde{u}}{\partial \nu_2} \Big|_+ = \varepsilon_+ \frac{\partial \tilde{u}}{\partial \nu_2} \Big|_- & \text{on } \partial D_2, \\ (\tilde{u} - \tilde{u}^i)(\zeta) = O(|\zeta - (1, 0)|) & \text{as } \zeta \rightarrow (1, 0), \end{cases}$$



(a) h_0 perturbation on the half-plane: $\partial\mathbb{H}_\delta$

(b) h perturbation on the unit disk: $\partial D_{1,\delta}$

Figure 3.1: The plasmonic particle (left, blue) and the perturbed half-plane (left, red) are transformed into concentric perturbed disks (right).

where $\tilde{\varepsilon} = \varepsilon_- \chi(D_1) + \varepsilon_+ \chi(D_2 \setminus \overline{D_1}) + \varepsilon_c \chi(\mathbb{R}^2 \setminus D_2)$ and $\frac{\partial}{\partial \nu_i}$ denotes the outward normal derivative with respect to ∂D_i for $i = 1, 2$.

The solution \tilde{u} can be represented by

$$\tilde{u} = \tilde{u}^i + \mathcal{S}_{D_1}[\phi_1] + \mathcal{S}_{D_2}[\phi_2], \quad (3.4)$$

where the densities ϕ_1 and ϕ_2 satisfy the system of integral equations

$$\begin{cases} \varepsilon_+ \frac{\partial}{\partial \nu_1} \left(\tilde{u}^i + \mathcal{S}_{D_1}[\phi_1] + \mathcal{S}_{D_2}[\phi_2] \right) \Big|_+ = \varepsilon_- \frac{\partial}{\partial \nu_1} \left(\tilde{u}^i + \mathcal{S}_{D_1}[\phi_1] + \mathcal{S}_{D_2}[\phi_2] \right) \Big|_- & \text{on } \partial D_1, \\ \varepsilon_c \frac{\partial}{\partial \nu_2} \left(\tilde{u}^i + \mathcal{S}_{D_1}[\phi_1] + \mathcal{S}_{D_2}[\phi_2] \right) \Big|_+ = \varepsilon_+ \frac{\partial}{\partial \nu_2} \left(\tilde{u}^i + \mathcal{S}_{D_1}[\phi_1] + \mathcal{S}_{D_2}[\phi_2] \right) \Big|_- & \text{on } \partial D_2, \end{cases} \quad (3.5)$$

or equivalently,

$$\begin{cases} (\lambda_{-+} I - \mathcal{K}_{D_1}^*)[\phi_1] = \frac{\partial}{\partial \nu_1} \left(\tilde{u}^i + \mathcal{S}_{D_2}[\phi_2] \right) & \text{on } \partial D_1, \\ (\lambda_{+c} I - \mathcal{K}_{D_2}^*)[\phi_2] = \frac{\partial}{\partial \nu_2} \left(\tilde{u}^i + \mathcal{S}_{D_1}[\phi_1] \right) & \text{on } \partial D_2, \end{cases} \quad (3.6)$$

with

$$\lambda_{-+} = \frac{\varepsilon_- + \varepsilon_+}{2(\varepsilon_- - \varepsilon_+)} \quad \text{and} \quad \lambda_{+c} = \frac{\varepsilon_+ + \varepsilon_c}{2(\varepsilon_+ - \varepsilon_c)}. \quad (3.7)$$

Since $|\lambda_{-+}| > \frac{1}{2}$ and $|\lambda_{+c}| < \frac{1}{2}$, the operator $(\lambda_{-+} I - \mathcal{K}_{D_1}^*)$ is invertible. Then we have from (3.6) that

$$\phi_1 = (\lambda_{-+} I - \mathcal{K}_{D_1}^*)^{-1} \frac{\partial}{\partial \nu_1} \left(\tilde{u}^i + \mathcal{S}_{D_2}[\phi_2] \right). \quad (3.8)$$

By substituting (3.8) into (3.6), we obtain the following result.

Proposition 3.1. *The density ϕ_2 on ∂D_2 satisfies the equation*

$$(\lambda_{+c} I - \mathcal{A})[\phi_2] = \frac{\partial \tilde{u}_{D_1}}{\partial \nu_2} \quad \text{on } \partial D_2,$$

where the operator \mathcal{A} is given by

$$\mathcal{A} := \mathcal{K}_{D_2}^* + \frac{\partial}{\partial \nu_2} \mathcal{S}_{D_1} (\lambda_{-+} I - \mathcal{K}_{D_1}^*)^{-1} \frac{\partial \mathcal{S}_{D_2}[\cdot]}{\partial \nu_1},$$

and

$$\tilde{u}_{D_1} := \tilde{u}^i + \mathcal{S}_{D_1}(\lambda_{-+}I - \mathcal{K}_{D_1}^*)^{-1} \left[\frac{\partial \tilde{u}^i}{\partial \nu_1} \right].$$

It can be shown that the operator \mathcal{A} is self-adjoint and compact [11]. So it has real eigenvalues and admits the following spectral decomposition:

$$\mathcal{A} = \sum_{n \in \mathbb{Z}} \lambda_n \varphi_n \otimes \varphi_n, \quad (3.9)$$

where (λ_n, φ_n) are the eigenvalue-eigenfunction pairs of the operator \mathcal{A} . It can also be shown that the eigenvalues satisfy $|\lambda_n| \leq 1/2$.

Now we discuss how to measure the plasmonic resonance frequency or the eigenvalues λ_n . One can see that, using (3.9), the polarizability p_Ω of the plasmonic particle Ω is given by

$$p_\Omega := \int_{\partial\Omega} u^i \psi_2 d\sigma = \sum_{n \in \mathbb{Z}} \frac{(\tilde{u}^i, \varphi_n)_{L^2(\partial D_2)} (\varphi_n, \frac{\partial \tilde{u}_{D_1}}{\partial \nu_2})_{\mathcal{H}^*(\partial D_2)}}{\lambda_{+c} - \lambda_n}, \quad (3.10)$$

where $\psi_2 = |\Phi'|^{-1}(\phi_2 \circ \Phi)$. The absorption cross section, which can be measured from the far-field region, by the small particle Ω is proportional to the imaginary part of the polarizability p_Ω in the quasi-static limit. Recalling the Drude model (2.9), we see that λ_{+c} depends on the frequency and satisfies $|\operatorname{Re} \lambda_{+c}| \leq 1/2$ for $\omega < \omega_p$. So, the particle's resonance frequencies and the corresponding eigenvalues λ_n can be measured as discussed in Subsection 2.2. From (3.10), it is clear that when we vary the frequency of the incident field, at the frequency ω_n such that $\lambda_{D_2}(\omega_n) = \lambda_n$ for some n which satisfies the condition

$$(\tilde{u}^i, \varphi_n)_{L^2(\partial D_2)} (\varphi_n, \frac{\partial \tilde{u}_{D_1}}{\partial \nu_2})_{\mathcal{H}^*(\partial D_2)} \neq 0,$$

the absorption cross section shows a sharp peak, which means that a plasmonic resonance is excited. In this way, we can measure the resonance frequency ω_n or the eigenvalue λ_n . In the next subsection, we analyze the asymptotic structure of the eigenvalue λ_n for small δ .

3.2 Asymptotic expansion of the operator \mathcal{A}

Here we compute an asymptotic expansion of the operator $\mathcal{A} : \mathcal{H}^*(\partial D_2) \rightarrow \mathcal{H}^*(\partial D_2)$ for small δ , where $\mathcal{H}^*(\partial D_2)$ is defined by (2.3) with D replaced by D_2 . Since $\partial D_{1,0}$ is the unit circle, we use the Fourier basis $\{e^{in\theta}\}_{n \neq 0}$ as a basis of $\mathcal{H}^*(\partial D_2)$. Let (r, θ) be the polar coordinates in the ζ -plane, i.e., $\zeta = re^{i\theta}$. Then the following proposition holds.

Proposition 3.2. *We have the following asymptotic expansion of the operator \mathcal{A} for small δ as follows: for $\zeta = e^{s+i\theta} \in \partial D_2$,*

$$\begin{aligned} \mathcal{A}[e^{in\theta}](\zeta) = & -\frac{1}{4\lambda_{-+}} e^{-2|n|s} e^{in\theta} \\ & - \delta \sum_{m \in \mathbb{Z} \setminus \{0\}} \frac{(\varepsilon_- |nm| + \varepsilon_+ nm)}{4|n|(\varepsilon_- - \varepsilon_+) \lambda_{-+}^2} e^{-(|n|+|m|)s} \hat{h}(-n+m) e^{im\theta} + O(\delta^2) \end{aligned}$$

for $n \neq 0$.

Proof. Following the same arguments as those in [11], we obtain

$$\begin{aligned}\mathcal{A}[\varphi_n^c](\zeta) &= \sum_{m=1}^{\infty} -\frac{1}{4\pi|n|} e^{-(|n|+m)s} [M_{nm}^{cc}(\lambda_{-+}, D_{1,\delta}) \varphi_m^c(\theta) + M_{nm}^{cs}(\lambda_{-+}, D_{1,\delta}) \varphi_m^s(\theta)], \\ \mathcal{A}[\varphi_n^s](\zeta) &= \sum_{m=1}^{\infty} -\frac{1}{4\pi|n|} e^{-(|n|+m)s} [M_{nm}^{sc}(\lambda_{-+}, D_{1,\delta}) \varphi_m^c(\theta) + M_{nm}^{ss}(\lambda_{-+}, D_{1,\delta}) \varphi_m^s(\theta)],\end{aligned}$$

for $\varphi_n^c(\theta) = \cos n\theta$, $\varphi_n^s(\theta) = \sin n\theta$, and $n \neq 0$. Then, by using the linearity of \mathcal{A} , it follows that

$$\begin{aligned}\mathcal{A}[e^{in\theta}](\zeta) &= \mathcal{A}[\varphi_n^c](\zeta) + i\mathcal{A}[\varphi_n^s](\zeta) \\ &= \sum_{m \in \mathbb{Z} \setminus \{0\}} -\frac{1}{8\pi|n|} e^{-(|n|+|m|)s} \mathbb{N}_{nm}^{(2)}(\lambda_{-+}, D_{1,\delta}) e^{im\theta}.\end{aligned}\quad (3.11)$$

We then decompose $\mathcal{A}[e^{in\theta}]$ as follows:

$$\begin{aligned}\mathcal{A}[e^{in\theta}](\zeta) &= \sum_{m \in \mathbb{Z} \setminus \{0\}} -\frac{1}{8\pi|n|} e^{-(|n|+|m|)s} \mathbb{N}_{nm}^{(2)}(\lambda_{-+}, D_{1,0}) e^{im\theta} \\ &\quad + \sum_{m \in \mathbb{Z} \setminus \{0\}} -\frac{1}{8\pi|n|} e^{-(|n|+|m|)s} [\mathbb{N}_{nm}^{(2)}(\lambda_{-+}, D_{1,\delta}) - \mathbb{N}_{nm}^{(2)}(\lambda_{-+}, D_{1,0})] e^{im\theta} \\ &:= I + II.\end{aligned}$$

Note that I is of order one but II is of order δ . First, we compute I . Since ∂D_1 and ∂D_2 are circles,

$$\mathcal{K}_{D_1}^*[e^{in\theta}] = \mathcal{K}_{D_2}^*[e^{in\theta}] = 0; \quad (3.12)$$

see, for instance, [2]. Moreover, from [1] it follows that

$$\frac{\partial}{\partial r} \mathcal{S}_B[e^{in\theta}](w) = \begin{cases} -\frac{1}{2} \left(\frac{r}{r_0}\right)^{|n|} e^{in\theta} & \text{if } |w| = r < r_0, \\ \frac{1}{2} \left(\frac{r_0}{r}\right)^{|n|} e^{in\theta} & \text{if } |w| = r > r_0, \end{cases} \quad (3.13)$$

where B is the disk centered at the origin and with radius r_0 . By using (3.12) and (3.13) (with B replaced by D_1 and D_2), we obtain

$$I = -\frac{1}{4\lambda_{-+}} e^{-2|n|s} e^{in\theta} \quad \text{for } n \neq 0.$$

We next consider II . From Lemma 2.1, it follows that

$$\begin{aligned}II &= -\frac{1}{4\lambda_{-+}} e^{-2|n|s} e^{in\theta} \\ &\quad - \delta \sum_{m \in \mathbb{Z} \setminus \{0\}} \frac{(\varepsilon_- |nm| + \varepsilon_+ nm)}{4|n|(\varepsilon_- - \varepsilon_+) \lambda_{-+}^2} e^{-(|n|+|m|)s} \hat{h}(-n+m) e^{im\theta} + O(\delta^2),\end{aligned}$$

which completes the proof. \square

Consequently, we can represent the approximation of \mathcal{A} in a matrix form as shown in the following result.

Corollary 3.3. *Let V_n be the subspace of $\mathcal{H}^*(\partial D_2)$ spanned by $\{e^{in\theta}, e^{-in\theta}\}$ for each $n \neq 0$. Then the operator $\mathcal{A} : \mathcal{H}^*(\partial D_2) \rightarrow \mathcal{H}^*(\partial D_2)$ can be represented in a block matrix form as follows:*

$$\begin{aligned} \mathcal{A} &= \begin{bmatrix} D_1 & & & \\ & \ddots & & \\ & & D_n & \\ & & & \ddots \end{bmatrix} + \delta \begin{bmatrix} H_{11} & H_{12} & H_{13} & \cdots \\ H_{21} & H_{22} & H_{23} & \cdots \\ H_{31} & H_{32} & H_{33} & \cdots \\ \vdots & \vdots & \vdots & \ddots \end{bmatrix} + O(\delta^2) \\ &=: \mathcal{A}_0 + \delta \mathcal{A}_1 + O(\delta^2). \end{aligned} \quad (3.14)$$

Here, the operators $D_n : V_n \rightarrow V_n$ and $H_{nm} : V_m \rightarrow V_n$ are represented in the following matrix forms using $\{e^{in\theta}, e^{-in\theta}\}$ as basis:

$$D_n = \begin{bmatrix} \lambda_{-n}^0 & 0 \\ 0 & \lambda_n^0 \end{bmatrix} \quad \text{with } \lambda_n^0 = -\frac{1}{4\lambda_{-+}} e^{-2|n|s}, \quad (3.15)$$

and

$$H_{nm} = -\frac{m}{4\lambda_{-+}^2} e^{-(|n|+|m|)s} \begin{bmatrix} 2\lambda_{-+}\hat{h}(-n+m) & \hat{h}(n+m) \\ \hat{h}(-n-m) & 2\lambda_{-+}\hat{h}(n-m) \end{bmatrix}, \quad (3.16)$$

for $n, m \in \mathbb{N}$.

The above result tells us that, in view of the eigenvalue perturbation theory [24], we see that the eigenvalues λ_n have the following asymptotic expansion:

$$\lambda_n = \lambda_n^0 + \delta \lambda_n^1 + O(\delta^2), \quad (3.17)$$

for some coefficient λ_n^1 . The eigenvalue λ_n^0 corresponds to the case of the unperturbed half-plane $\partial \mathbb{H}_0$. In the case of the perturbed half-plane $\partial \mathbb{H}_\delta$, the eigenvalue λ_n is slightly different from λ_n^0 . The difference is called the shift of the eigenvalues. This shift is due to the interaction of the target particle with the plasmonic particle. As already explained in the previous subsection, we can measure the values of the eigenvalues λ_n . Since we know λ_n^0 explicitly from (3.15), we can also measure the shift of the eigenvalues $\lambda_n - \lambda_n^0 \approx \delta \lambda_n^1$. It is natural to expect that these shifts contain information on the shape of the perturbed half-plane $\partial \mathbb{H}_\delta$. In the next section, we discuss how to reconstruct the shape of $\partial \mathbb{H}_\delta$ from these recovered eigenvalues.

4 The reconstruction problem

Our aim in this section is to reconstruct the shape of the small perturbation δh_0 of the half-space $\partial \mathbb{H}_\delta$ using the plasmonic resonances of the small particle Ω .

We assume that we measured the plasmonic eigenvalues λ_n of the operator \mathcal{A} for $n = 1, 2, \dots, N$ from the far field by varying the frequency of the incident field and then picking up local peaks. Then, we can also measure the shift $\lambda_n - \lambda_n^0 \approx \delta \lambda_n^1$ as explained in Subsection 3.2. In Proposition 4.1, we provide an explicit formula for the Fourier coefficients of the perturbation δh of the transformed half-plane ∂D_1 in terms of the shift $\delta \lambda_n^1$. This formula can be used to reconstruct the perturbation δh in a direct way. Once δh is

reconstructed, the perturbation of the planar surface δh_0 can be determined by inverting the conformal map Φ and constructing $\Phi^{-1}(D_{1,\delta})$.

The following result holds.

Proposition 4.1. *Let h be the real-valued function in (3.3). We further assume that h is an even function. We have, for $n = 1, 2, 3, \dots$,*

$$\operatorname{Re}\{\hat{h}(2n)\} = -\frac{2\lambda_{-+}^2(\lambda_n^1 - \lambda_{-n}^1)}{n}e^{-2ns}, \quad \operatorname{Im}\{\hat{h}(2n)\} = 0,$$

and

$$\hat{h}(0) = -\lambda_{-+}(\lambda_1^1 + \lambda_{-1}^1)e^{-2s}.$$

Note that, since h is an even function, we have $\hat{h}(2n-1) = 0$ and $\hat{h}(-n) = \hat{h}(n)$.

Proof. We first derive the asymptotic expansion of the eigenvalues of the operator \mathcal{A} for small δ . In what follows, by abuse of notation, we shall identify the operators $\mathcal{A}, \mathcal{A}_0$ and \mathcal{A}_1 with their matrix representation. Let us denote the standard inner product in $\ell^2(\mathbb{Z})$ by $\langle \cdot, \cdot \rangle$. Let us denote by v_n the eigenvector corresponding to the eigenfunction of the operator \mathcal{A} . Also, let $\{v_n^0\}_{n \in \mathbb{Z}}$ be the standard orthonormal basis of $\ell^2(\mathbb{Z})$. Note that $v_n^0, n \in \mathbb{Z}$, is an eigenvector of the matrix \mathcal{A}_0 .

We first observe that the unperturbed matrix \mathcal{A}_0 has degenerate eigenvalues λ_n^0 with two associated eigenvectors v_n^0 and v_{-n}^0 . So, by applying a standard argument of the degenerate eigenvalue perturbation theory to the expansion (3.14), we see that the asymptotics of the eigenvector associated to the eigenvalue λ_n has the following form:

$$v_n = \alpha_n v_n^0 + \beta_n v_{-n}^0 + O(\delta), \quad (4.1)$$

for some coefficients α_n and β_n . Note that the leading order term is a linear combination of the eigenvectors v_n^0, v_{-n}^0 of the unperturbed matrix \mathcal{A}_0 .

By applying (3.14), (3.17) and (4.1) to $\mathcal{A}v_n = \lambda_n v_n$, we have, up to $O(\delta^2)$,

$$(\mathcal{A}_0 + \delta \mathcal{A}_1)(\alpha_n v_n^0 + \beta_n v_{-n}^0 + \delta v_n^1) = (\lambda_n^0 + \delta \lambda_n^1)(\alpha_n v_n^0 + \beta_n v_{-n}^0 + \delta v_n^1),$$

which yields the following equation by matching the first order terms with respect to δ :

$$\mathcal{A}_0 v_n^1 + \alpha_n \mathcal{A}_1 v_n^0 + \beta_n \mathcal{A}_1 v_{-n}^0 = \lambda_n^0 v_n^1 + \alpha_n \lambda_n^1 v_n^0 + \beta_n \lambda_n^1 v_{-n}^0. \quad (4.2)$$

Then, by taking the inner product with v_n^0 and applying (3.14), we obtain

$$\begin{aligned} \alpha_n \lambda_n^1 &= \alpha_n \langle v_n^0, \mathcal{A}_1 v_n^0 \rangle + \beta_n \langle v_n^0, \mathcal{A}_1 v_{-n}^0 \rangle \\ &= |k| \frac{\lambda_n^0}{\lambda_{-+}} \left[2\alpha_n \lambda_{-+} \hat{h}(0) + \beta_n \hat{h}(-2n) \right] \\ &= |k| \frac{\lambda_n^0}{\lambda_{-+}} \left[2\alpha_n \lambda_{-+} \hat{h}(0) + \beta_n \overline{\hat{h}(2n)} \right], \end{aligned} \quad (4.3)$$

Similarly, taking the inner product with v_{-n}^0 yields

$$\begin{aligned} \beta_n \lambda_n^1 &= \alpha_n \langle v_{-n}^0, \mathcal{A}_1 v_n^0 \rangle + \beta_n \langle v_{-n}^0, \mathcal{A}_1 v_{-n}^0 \rangle \\ &= |n| \frac{\lambda_n^0}{\lambda_{-+}} \left[\alpha_n \hat{h}(2n) + 2\beta_n \lambda_{-+} \hat{h}(0) \right], \end{aligned} \quad (4.4)$$

where λ_n^0 is given in (3.15). Rewriting (4.3) and (4.4) in a matrix form, we arrive at the following eigenvalue problem for λ_n^1 :

$$|n| \frac{\lambda_n^0}{\lambda_{-+}} \begin{bmatrix} 2\lambda_{-+}\hat{h}(0) & \hat{h}(2n) \\ \hat{h}(2n) & 2\lambda_{-+}\hat{h}(0) \end{bmatrix} \begin{bmatrix} \alpha_n \\ \beta_n \end{bmatrix} = \lambda_n^1 \begin{bmatrix} \alpha_n \\ \beta_n \end{bmatrix}.$$

Solving this eigenvalue problem yields

$$\lambda_{\pm n}^1 = |n| \lambda_0^{|n|} \left(2\hat{h}(0) \pm \frac{1}{\lambda_{-+}} \hat{h}(\pm 2n) \right). \quad (4.5)$$

Note that, since h is an even function, the imaginary part of every Fourier coefficient $\hat{h}(n)$ vanishes. So, we have from (2.20) that $\hat{h}(-n) = \overline{\hat{h}(n)} = \hat{h}(n)$. Therefore, (4.5) becomes

$$\lambda_{\pm n}^1 = |n| \lambda_{|n|}^0 \left(2\hat{h}(0) \pm \frac{1}{\lambda_{-+}} \hat{h}(2n) \right). \quad (4.6)$$

Then the conclusion follows from rearranging the terms with (3.15). \square

Remark 1. *For the reconstruction of more general-shaped perturbations, we should be able to reconstruct the odd Fourier coefficients of h . These coefficients are contained in the second order terms in the asymptotic expansion for the eigenvalues of \mathcal{A} . So if the signal-to-noise ratio in the measurements is large enough, it would be possible to reconstruct the odd coefficients. The derivation of the second order term and a more complete reconstruction scheme will be considered elsewhere.*

5 Numerical examples

In this section, we present numerical examples to support the theoretical results. We assume that the measurements of the eigenvalues λ_j are accurate. We generate the eigenvalues data as follows. We construct a truncated matrix for the operator \mathcal{A} using formula (3.11) which is written in terms of the CGPTs. To compute these CGPTs for the transformed shape $D_{1,\delta}$, we discretize the boundary integral in (2.11) using the trapezoidal rule. We use 300 equispaced points for the discretization of the boundary $\partial D_{1,\delta}$. By computing the eigenvalue of the resulting matrix for \mathcal{A} , we can obtain accurate approximations of the eigenvalues λ_n . Then, as described in Section 4, we reconstruct the shape of $\partial D_{1,\delta}$ and hence that of the perturbed half-plane $\partial \mathbb{H}_\delta$.

We shall consider the case when the perturbation δh of the planar surface is an even function. Then all the odd Fourier coefficients $\hat{h}(2n-1)$ are zero. From Proposition 4.1, we recover even Fourier coefficients of h . Hence, in view of (2.20), we reconstruct h from the following truncated Fourier series:

$$h_{\text{eig}}(\theta) = \sum_{k=-\frac{N}{2}}^{\frac{N}{2}} \hat{h}(2k) e^{i2k\theta} = \hat{h}(0) + 2 \sum_{k=1}^{\frac{N}{2}} \Re[\hat{h}(2k)] \cos(2k\theta) - 2 \sum_{k=1}^{\frac{N}{2}} \Im[\hat{h}(2k)] \sin(2k\theta).$$

We compare the reconstructed images to those obtained from the complex GPTs. The CGPTs can be measured from the far field measurements, see [4]. It is worth mentioning

that the reconstruction of the higher order CGPTs is very sensitive to measurement noise. We reconstruct the Fourier coefficients of h from the CGPTs by using the Proposition 2.1.

In the reconstruction of h using the complex GPTs, we truncate the Fourier series of order N and use (2.20) to arrive at

$$h_{GPT}(\theta) = \sum_{k=-N}^N \hat{h}(k) e^{ik\theta} = \hat{h}(0) + 2 \sum_{k=1}^N \Re[\hat{h}(k)] \cos(k\theta) - 2 \sum_{k=1}^N \Im[\hat{h}(k)] \sin(k\theta).$$

In what follows, we present two numerical examples for validation of our approach. For their detailed implementations using MATLAB, we refer to [33, 34].

5.1 Example 1

We set $\delta = 10^{-2}$, $d = 1.04$, and $R = 0.4$. Moreover, we assume $\epsilon_- = 3$ and $\epsilon_+ = 1$. Then we get $\lambda_{-+} = 1$ from (3.7). Let I be the union of the intervals given by

$$I = [-0.7R, -0.5R] \cup [-0.3R, -0.1R] \cup [0.1R, 0.3R] \cup [0.5R, 0.7R].$$

We define $h_0 : \mathbb{R} \rightarrow \mathbb{R}$ as the following even function:

$$h_0(x) = \begin{cases} -1 & \text{for } x \in I, \\ 0 & \text{for } x \in \mathbb{R} \setminus I. \end{cases} \quad (5.1)$$

Recalling

$$\partial\mathbb{H}_\delta = \{\mathbf{x} + \delta h_0(\mathbf{x}) \nu(\mathbf{x}) : \mathbf{x} \in \partial\mathbb{H}_0\},$$

we see that the shape of the perturbed surface $\partial\mathbb{H}_\delta$ is a corrugated plane.

Figures 5.1a and 5.1c show the results of the reconstruction of the perturbation δh_0 based on GPTs and the shift of plasmon resonances, respectively. By transforming $\partial D_{1,\delta}$ to $\partial\mathbb{H}_\delta$ using Φ^{-1} , we obtain the reconstructed δh_0 as illustrated in Figures 5.1b and 5.1d.

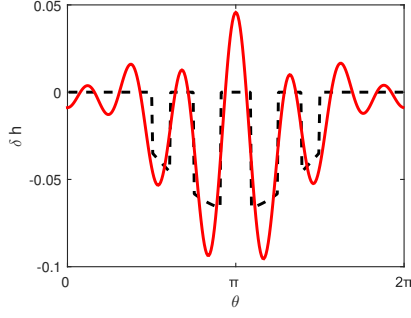
5.2 Example 2

For the second example, we set $\delta = 10^{-1}$, $d = 2$ and $R = 0.8$. Moreover, we put $\epsilon_- = 3$ and $\epsilon_+ = 1$, so we have $\lambda_{-+} = 1$ from (3.7). We now define $h_0 : \mathbb{R} \rightarrow \mathbb{R}$ as a smooth even function:

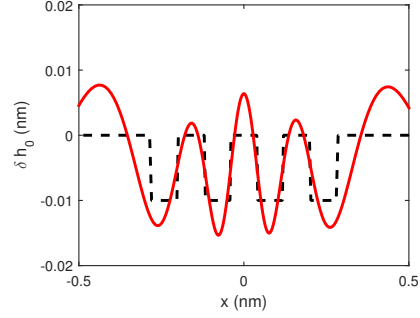
$$h_0(x) = - \left[e^{-(\frac{x}{R}+2)^2} + e^{-(\frac{x}{R}-2)^2} \right].$$

The reconstructed shapes of δh from the CGPTs and the shifts of the eigenvalues are shown in Figures 5.2a and 5.2c, respectively. By transforming $\partial D_{1,\delta}$ to $\partial\mathbb{H}_0$ applying Φ^{-1} , we finally reconstruct δh_0 as shown in Figures 5.2b and 5.2d.

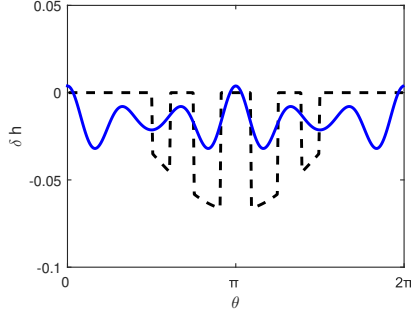
In contrast with the red line in Figure 5.1a, the blue line in Figure 5.1c shows very large fluctuations at both left and right extremities. Moreover, in comparison to the blue line in Figure 5.2c, the red line in Figure 5.2a is much more flat at both left and right extremities. These phenomena are due to the lack of odd Fourier coefficients in δh_{eig} . Nevertheless, even Fourier coefficients of δh contain comprehensive information of $\partial\mathbb{H}_\delta$.



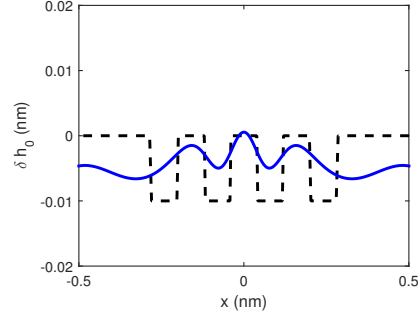
(a) Reconstruction of δh by the GPTs.



(b) Reconstruction of δh_0 by the GPTs.



(c) Reconstruction of δh by the eigenvalues.

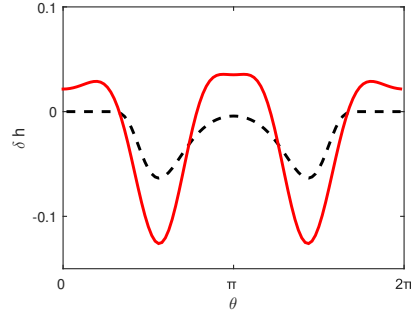


(d) Reconstruction of δh_0 by the eigenvalues.

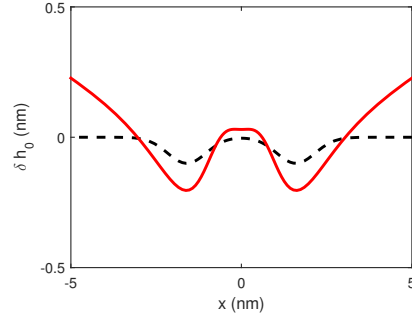
Figure 5.1: The dotted lines are the theoretical $\delta h : [0, 2\pi] \rightarrow \mathbb{R}$ and $\delta h_0 : \mathbb{R} \rightarrow \mathbb{R}$, the red lines are the reconstruction of δh and δh_0 using the complex GPTs, and the blue lines are the reconstruction of δh and δh_0 using the eigenvalue perturbations. In this case, $N = 8$.

6 Concluding remarks

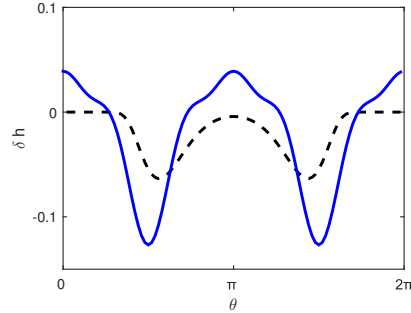
In this paper, we have introduced an original approach to recover small perturbations of a planar surface from shifts in the resonances of the plasmonic particle-surface system. Our main idea is to design a conformal mapping which transforms the particle-surface system into a coated structure, in which the inner core corresponds to the local perturbations of the planar surface. Then we have related the perturbations of the plasmonic resonances to the Fourier coefficients of the transformed perturbations. Using these (approximate) relations, we have designed a direct (non-iterative) scheme for retrieving the perturbations of the planar surface. We have shown that only even coefficients of the Fourier coefficients of the transformed perturbations can be reconstructed from the leading-order terms of the resonances. For large enough signal-to-noise ratio in the measurements, we may be able to recover both the odd coefficients and the complex GPTs from second-order terms in the resonances and therefore, achieve better resolution. This would be the subject of a forthcoming work.



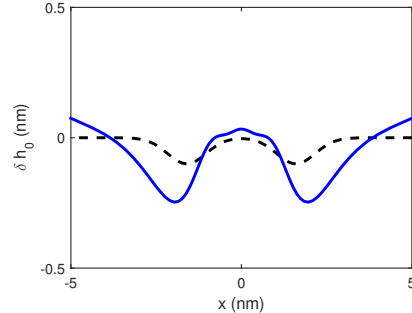
(a) Reconstruction of δh by the GPTs.



(b) Reconstruction of δh_0 by the GPTs.



(c) Reconstruction of δh by the eigenvalues.



(d) Reconstruction of δh_0 by the eigenvalues.

Figure 5.2: The dotted lines are the theoretical $\delta h : [0, 2\pi] \rightarrow \mathbb{R}$ and $\delta h_0 : \mathbb{R} \rightarrow \mathbb{R}$, the red lines are the reconstruction of δh and δh_0 using the complex GPTs, and the blue lines are the reconstruction of δh and δh_0 using the eigenvalue perturbations. Here, $N = 6$.

References

- [1] H. Ammari, G. Ciraolo, H. Kang, H. Lee, and G.W. Milton, Spectral theory of a Neumann-Poincaré-type operator and analysis of cloaking due to anomalous localized resonance, *Arch. Ration. Mech. Anal.*, 208 (2013), no. 2, 667–692.
- [2] H. Ammari, J. Garnier, W. Jing, H. Kang, M. Lim, K. Sølna, and H. Wang, *Mathematical and Statistical Methods for Multistatic Imaging*, Lecture Notes in Mathematics, Vol. 2098, Springer, Cham, 2013.
- [3] H. Ammari, J. Garnier, H. Kang, M. Lim, and S. Yu, Generalized polarization tensors for shape description, *Numer. Math.*, 126 (2014), 199–224.
- [4] H. Ammari and H. Kang, *Polarization and Moment Tensors with Applications to Inverse Problems and Effective Medium Theory*, Applied Mathematical Sciences, Vol. 162, Springer-Verlag, New York, 2007.
- [5] H. Ammari and H. Kang, Generalized polarization tensors, inverse conductivity problems, and dilute composite materials: a review, *Contemporary Mathematics*, Volume 408 (2006), 1–67.

- [6] H. Ammari, H. Kang, E. Kim, and J.-Y. Lee, The generalized polarization tensors for resolved imaging Part II: Shape and electromagnetic parameters reconstruction of an electromagnetic inclusion from multistatic measurements, *Math. Comp.*, 81 (2012), 839–860.
- [7] H. Ammari, H. Kang, M. Lim, and H. Zribi, The generalized polarization tensors for resolved imaging. Part I: Shape reconstruction of a conductivity inclusion, *Math. Comp.*, 81 (2012), 367–386.
- [8] H. Ammari, P. Millien, M. Ruiz, and H. Zhang, Mathematical analysis of plasmonic nanoparticles: the scalar case, *Arch. Ration. Mech. Anal.*, 224 (2017), 597–658.
- [9] H. Ammari, M. Ruiz, S. Yu, and H. Zhang, Mathematical analysis of plasmonic resonances for nanoparticles: the full Maxwell equations, *J. Differential Equations*, 261 (2016), 3615–3669.
- [10] H. Ammari, M. Ruiz, S. Yu, and H. Zhang, Reconstructing fine details of small objects by using plasmonic spectroscopic data, *SIAM J. Imaging Sci.*, 11 (2018), 1–23.
- [11] H. Ammari, M. Ruiz, S. Yu, and H. Zhang, Reconstructing fine details of small objects by using plasmonic spectroscopic data. Part II: The strong interaction regime, to appear in *SIAM J. Imaging Sci.*
- [12] H. Ammari and H. Zhang, A mathematical theory of super-resolution by using a system of sub-wavelength Helmholtz resonators, *Comm. Math. Phys.*, 337 (2015), 379–428.
- [13] H. Ammari and H. Zhang, Super-resolution in high contrast media, *Proc. Royal Soc. A*, 2015 (471), 20140946.
- [14] H. Ammari and H. Zhang, Effective medium theory for acoustic waves in bubbly fluids near Minnaert resonant frequency, *SIAM J. Math. Anal.*, 49 (2017), 3252–3276.
- [15] K. Ando and H. Kang, Analysis of plasmon resonance on smooth domains using spectral properties of the Neumann-Poincaré operator, *J. Math. Anal. Appl.*, 435 (2016), 162–178.
- [16] K. Ando, H. Kang, and H. Liu, Plasmon resonance with finite frequencies: a validation of the quasi-static approximation for diametrically small inclusions, *SIAM J. Appl. Math.*, 76 (2016), 731–749.
- [17] G. Bao, P. Li, and Y. Wang, Near-field imaging with far-field data, *Appl. Math. Lett.*, 60 (2016), 36–42.
- [18] A. Bouhelier, J. Renger, M.R. Beversluis, and L. Novotny, Plasmon-coupled tip-enhanced near-field optical microscopy, *J. Microsc.*, 210 (2003), 220–224.
- [19] P.S. Carney and J.C. Schotland, Near-field tomography. *Inside out: inverse problems and applications*, 133–168, *Math. Sci. Res. Inst. Publ.*, 47, Cambridge Univ. Press, Cambridge, 2003.

- [20] D. Courjon, *Near-Field Microscopy and Near-Field Optics*, Imperial College, 2003.
- [21] N. Garcia and M. Nieto-Vesperinas, Near-field optics inverse-scattering reconstruction of reflective surfaces, *Opt. Lett.*, 24 (1993), 2090–2092.
- [22] C. Girard and A. Dereux, Near-field optics theories, *Rep. Progr. Phys.*, 59 (1996), 657–699.
- [23] J.-J. Greffet and R. Carminati, Image formation in near-field optics, *Progr. Surface Sci.*, 56 (1997), 133–237.
- [24] T. Kato, *Perturbation Theory of Linear Operators*, Springer-Verlag, 1980.
- [25] S. Kawata, editor, *Near-Field Optics and Surface Plasmon Polaritons*, Topics in Applied Physics, Vol. 81, Springer, Berlin, 2001.
- [26] O.D. Kellogg, *Foundations of Potential Theory*, Dover, New-York, 1953.
- [27] K.L. Kelly, E. Coronado, L.L. Zhao, and G.C. Schatz, The optical properties of metal nanoparticles: The influence of size, shape, and dielectric environment, *J. Phys. Chem. B*, 107 (2003), 668–677.
- [28] D. Khavinson, M. Putinar, and H.S. Shapiro, Poincaré’s variational problem in potential theory, *Arch. Ration. Mech. Anal.*, 185 (2007) 143–184.
- [29] S. Link and M.A. El-Sayed, Shape and size dependence of radiative, non-radiative and photothermal properties of gold nanocrystals, *Int. Rev. Phys. Chem.*, 19 (2000), 409–453.
- [30] L. Novotny, The history of near-field optics, *Progress in Optics* 50, 137–180, E. Wolf (ed.), Elsevier, Amsterdam (2007).
- [31] L. Novotny and S.J. Stranick, Near-field optical microscopy and spectroscopy with pointed probes, *Ann. Rev. Phys. Chem.*, 57 (2006), 303–331.
- [32] L.B. Scaffardi and J.O. Tocho, Size dependence of refractive index of gold nanoparticles, *Nanotech.*, 17 (2006), 1309–1315.
- [33] D. S. Choi, https://matlab.mathworks.com/users/john72531/Published/h_reconstruction1/index.html
- [34] D. S. Choi, https://matlab.mathworks.com/users/john72531/Published/h_reconstruction2/index.html